Ocean Dynamics (2005) 55: 162–177
DOI 10.1007/s10236-005-0005-6

Jinyu Sheng · Richard J. Greatbatch
Xiaoming Zhai · Liqun Tang

A new two-way nesting technique for ocean modeling based on the smoothed semi-prognostic method

Received: 24 August 2004 / Accepted: 20 March 2005 / Published online: 25 October 2005

Abstract A new two-way nesting technique is presented for a multiple nested-grid ocean modeling system. The new technique uses the smoothed semi-prognostic (SSP) method to exchange information between the different subcomponents of the nested-grid system. Four versions of the new nesting technique are described, together with conventional one-way nesting. The performance of the different nesting techniques is compared, using two independent nested-grid modeling systems, one for the Scotian Shelf of the northwest Atlantic Ocean and the other for the Meso-American Barrier Reef System of the northwestern Caribbean Sea. Nesting using the semi-prognostic method is shown to effectively prevent unrealistic drift of the inner model, while use of the SSP method avoids unnecessary damping of small scales on the inner model grid. Comparison of the annual-mean flow field with the near-surface currents determined by Fratantoni (in J Geophys Res 106:2977–2996, 2001) from observed trajectories of near-surface drifters demonstrates the overall superiority of the nesting technique based on the SSP method.

Keywords Two-way nesting · Semi-prognostic method · Ocean model · Shelf circulation · Scotian Shelf · Meso-American Barrier Reef System

1 Introduction

Ocean circulation models have increasingly been used to simulate circulation and temperature/salinity (T/S) distributions in the ocean, and can be broadly categorized in terms of the numerical methods and model grids used in the model development. The four basic numerical methods (see Durran 1999; Griffies et al. 2000; Jones 2002) are the finite difference method (e.g. the model used here; see Sheng et al. 1998), the finite element method (e.g. Le Provost et al. 1994), the finite volume method (e.g. Marshall et al. 1997), and the Galerkin-spectral method (e.g. Haidvogel et al. 1991). The commonly used model grids are structured grids (the model grid cells have the same number of sides and neighboring cells), unstructured grids (the model grid cells take nonuniform geometrical shapes) and adaptive grids (the model grid cells evolve with the flow, e.g. Pain 2000). The unstructured and adaptive grid models have the advantage of resolving complex geometries and flows with large spatial variations and are particularly useful for simulating circulation in regions of complex coastal geometry or steep bottom topography. The unstructured grid, however, has difficulty to represent the geostrophic balance and is computationally expensive (Griffies et al. 2000). In addition, a nonuniform model grid provides an opportunity for unphysical wave scattering. Therefore, the majority of ocean circulation model studies to date have used the finite difference/finite volume method with uniform grids.

It is, however, a formidable task to fully resolve physical processes that operate in the ocean on various temporal and spatial scales using a numerical model with a uniform grid. Usually, one is faced with a choice between a basin-scale simulation at a relatively coarse resolution to resolve mainly the large-scale circulation features or a regional-scale simulation with a very high resolution to resolve small-scale features such as fronts and eddies within a limited area domain. In a limited-area simulation, a prior knowledge is required to describe physical processes at work along model open boundaries, and interaction between the basin-scale, used to prescribe the boundary conditions, and the smaller-scale circulation within the model domain are prohibited. Sometimes a large-scale model contains choke points (such as the Gulf Stream separation region) where a very high-resolution simulation would be an

Responsible Editor: Phil Dyke

J. Sheng (✉) · R. J. Greatbatch · X. Zhai · L. Tang
Department of Oceanography,
Dalhousie University, Halifax, NS, Canada, B3H 4J1
E-mail: jinyu.sheng@dal.ca
Tel.: +1-902-4942718
Fax: +1-902-4942885

advantage, although such high resolution is not required over the rest of the domain. In such circumstances, a nested-grid modeling system may be advantageous, in which a finer-resolution inner model is embedded inside a coarser-resolution outer model. Indeed, the main advantage of a nested-grid modeling system is to increase the model resolution in subregions to resolve fine-scale circulation features without having the computational expense of using high-resolution over the whole model domain (Fox and Maskell 1995).

In the past, two basic approaches have been used to exchange information between the subcomponents of a nested-grid modeling system. The first is conventional one-way (C1W) nesting in which a fine-resolution inner model is connected to a coarser-resolution outer model only through the specification of the open boundary conditions for the inner model, these being taken from the outer model-computed fields. The main advantage of C1W nesting is that the outer and inner models can be run sequentially and it is therefore computationally efficient. There are two main disadvantages. First, there is no constraint from the outer model on the interior of the inner model domain. This can lead to drift of the inner model and result in a flow field in the inner model that differs radically from that in the outer model (a comparison of Fig. 3a, f, discussed in detail in Sect. 3, illustrates this problem). Second, C1W nesting does not allow feedback from the inner model to the outer model with the result that the outer model does not benefit from the finer resolution within the inner model domain.

The second approach to nesting allows for two-way interaction between the subcomponents of a nested modeling system, in addition to the specification of open boundary conditions for the inner model based on the outer model fields. Two-way interaction can be achieved in many ways. A commonly used technique is to transfer information between the two grids at a narrow zone (or dynamic interface) near the grid interface (Kurihara et al. 1979; Ginis et al. 1998). The coarse-grid model variables, such as currents, T/S and associated fluxes at the dynamic interface are interpolated onto the fine grid to provide time-dependent boundary conditions for the fine grid, and the fine-grid model variables are interpolated back onto the coarse grid to update the coincident coarse-grid values at the dynamic interface. It should be noted that the dynamic interface of this nesting scheme can be considered as an internal boundary for the coarse-grid model, and the coarse-grid integration is not necessary over the subregion covered by the fine-grid domain. Clearly, a possible disadvantage of this method is that, as in C1W nesting, the outer model does not constrain the interior of the inner model domain directly, and, hence, there is nothing to prevent unrealistic drift of the inner model.

An alternative two-way nesting technique, suggested by Oey and Chen (1992), is to embed a fine-resolution inner model inside a coarser-resolution outer model and use the inner model variables to replace the outer model variables over the subregion where the two grids overlap. This two-way nesting technique has the advantage of allowing a two-way interaction at the grid interface, and also allows the outer model to benefit directly from the finer resolution of the inner model where the two grids overlap. Nevertheless, there is still no direct constraint on the evolution of the inner model within the interior of its domain.

The new technique to be presented here is similar to Oey and Chen (1992) in that a fine-grid inner model is embedded inside a coarser-grid outer model. Different from Oey and Chen's nesting approach, we use the smoothed semi-prognostic (SSP) method (Eden et al. 2004; Greatbatch et al. 2004) to exchange information between the interiors of inner and outer models where their domains overlap. An advantage of semi-prognostic nesting is that the inner and outer models are always coupled throughout their region of overlap, so that drift of the inner model, independent of the outer model, is effectively eliminated. It should be noted that the new nesting technique can easily be applied to a multiply nested-grid modeling system with one or more fine-resolution inner models embedded inside a coarser-grid outer model, and one or more finer-resolution local submodels embedded inside each inner model, and so on.

The arrangement of this paper is as follows: Sect. 2 describes the new two-way nesting technique based on the SSP method. Sections 3 and 4 discuss the performance of the new nesting technique using two independent nested-grid modeling systems, one for the Scotian Shelf of the northwest Atlantic Ocean and the other for the Meso-American Barrier Reef System of the northwestern Caribbean Sea. The final section gives a summary and conclusions. We also include an Appendix where two test experiments are described in which the inner and outer models have the same resolution.

2 A new two-way nesting technique based on the SSP method

The unique feature of the new two-way nesting technique is the use of the SSP method (Eden et al. 2004; Greatbatch et al. 2004) to exchange information between the subcomponents of a nested-grid modeling system. The SSP method is a modification of the original semi-prognostic method (OSP) (as introduced by Sheng et al. (2001)), to eliminate damping on small scales (e.g. the mesoscale). The original application of both the OPS and SSP methods was to provide a simple way to adjust a model for systematic error (see Greatbatch et al. (2004) for a comprehensive overview). Indeed, the semi-prognostic method is closely related to the "pressure-correction method" described by Bell et al. (2004), and which is also a technique to correct for systematic bias in a model. In the semi-prognostic method, the adjustment is accomplished by replacing the density variable ρ in the model's hydrostatic equation by a linear combination of the model-computed density ρ_m and an input density ρ_c:

$$\rho = \alpha\rho_m + (1-\alpha)\rho_c, \tag{1}$$

where α is the linear combination coefficient with a value between 0 and 1. In Sheng et al. (2001), the input density ρ_c is computed from a monthly mean climatology of hydrographic data, but it might also be the density from another model, as in the nesting technique to be described here.

The hydrostatic equation

$$\frac{\partial p}{\partial z} = -g\rho_m - g(1-\alpha)(\rho_c - \rho_m), \tag{2}$$

where the second term on the right hand side of the above equation is the correction term used to correct for model systematic error and unresolved processes. Equation 2 is the form of the OSP method introduced by Sheng et al. (2001). As stated in Sheng et al. (2001), the above procedure is equivalent to adding a forcing term to the horizontal momentum equations (see also Greatbatch et al. 2004). This can be demonstrated by decomposing the model pressure p into two terms:

$$p = p^* + \hat{p}, \tag{3}$$

where p^* is the traditional pressure variable satisfying

$$\frac{\partial p^*}{\partial z} = -g\rho_m \tag{4}$$

with $p^* = g\rho_0\eta$ at the sea surface, and $\hat{p}$ is a correction term satisfying

$$\frac{\partial \hat{p}}{\partial z} = -g(1-\alpha)(\rho_c - \rho_m) \tag{5}$$

with $\hat{p} = 0$ at the sea surface. Using Eq. 3, the horizontal momentum equations can be rewritten as:

$$\frac{\partial \vec{u}}{\partial t} = -\frac{1}{\rho_o}\nabla_h p^* - \frac{1}{\rho_o}\nabla_h \hat{p} + \cdots, \tag{6}$$

where $\vec{u}$ is the horizontal velocity vector and ∇_h is the horizontal Laplacian operator. Therefore, the semi-prognostic method is equivalent to adding a body forcing term $(-\frac{1}{\rho_o}\nabla_h\hat{p})$ to the model horizontal momentum equations. It is important to note that the semi-prognostic method is adiabatic, leaving the temperature and salinity equations unadjusted (Greatbatch et al. 2004). Therefore, the semi-prognostic method makes no compromise to the requirement that the flow be primarily in the neutral tangent plane (see McDougall 1987) in the ocean interior, and the method is well-suited for use in tracer studies (e.g. Zhao et al. 2004).

The OSP method, however, has the drawback that it damps the mesoscale eddy field. Eden et al. (2004) introduced the smoothed semi-prognostic method (SSP) by applying the correction term only on large spatial scales:

$$\frac{\partial p}{\partial z} = -g\rho_m - g(1-\alpha)\langle\rho_c - \rho_m\rangle, \tag{7}$$

where $<\ >$ represents the spatial averaging. Eden et al. (2004) demonstrated that the SSP method is effective at eliminating the damping effect of the OSP method on the mesoscale eddy field.

If the input density ρ_c in Eq. 2 is the density from another model, the semi-prognostic method becomes a technique for transferring information into and between models (effectively "assimilating" data from one model to the other). As such, the semi-prognostic method can be used to construct a two-way interactive nesting technique for a nested-grid ocean circulation modeling system to be described as follows.

For the convenience of the presentation in this paper, we consider a simple nested-grid modeling system in which a high-resolution inner model is embedded inside a coarser-resolution outer model. In addition to the use of the outer model-computed fields to specify open boundary conditions for the inner model, the new two-way nesting technique (referred to as the SSP nesting technique) consists of the following two steps. First, the outer model density ρ_{outer} in the overlapping subregion is used to adjust the inner model based on

$$\frac{\partial p_{\text{inner}}}{\partial z} = -g\rho_{\text{inner}} - g(1-\beta_i)\langle\hat{\rho}_{\text{outer}} - \rho_{\text{inner}}\rangle \quad \text{(for the inner model)}, \tag{8}$$

where p_{inner} is the pressure variable of the inner model, ρ_{inner} is the inner model density, $\hat{\rho}_{\text{outer}}$ is density calculated from the outer model T/S fields after interpolation onto the inner model grid, β_i is a linear combination coefficient with a value between 0 and 1, and $<\ >$ is the smoothing operator. The use of the smoothing operator ensures that the inner model is constrained by the outer model only on large scales (determined by the smoothing scale that is used), the smaller scales associated with the fine grid of the inner model being free to evolve without constraint.

Second, the inner model density in the overlapping subregion is used to adjust the outer model in the same overlapping subregion based on

$$\frac{\partial p_{\text{outer}}}{\partial z} = -g\rho_{\text{outer}} - g(1-\beta_o)\langle\hat{\rho}_{\text{inner}} - \rho_{\text{outer}}\rangle \quad \text{(for the outer model)}, \tag{9}$$

where p_{outer} is the pressure variable of the outer model, ρ_{outer} is the outer model density, $\hat{\rho}_{\text{inner}}$ is density calculated from the inner model T/S fields after interpolation onto the outer model grid, β_o is a linear combination coefficient with a value between 0 and 1, and $<\ >$ is a smoothing operator, which is usually different from that in Eq. 8. Indeed, the smoothing operator in Eq. 9 can be chosen so that the correction term applies only on small scales (rather than only on large scales, as in Eq. 8), in which case, the operator $<\ >$ in Eq. 9 is really the inverse of a smoothing operator. For the present application, the second smoothing operator is not used.

It can be seen from Eqs. 8 and 9 that the new two-way nesting technique based on the SSP method is easy and straightforward to implement, since only the hydrostatic equations of the subcomponents of the nested-grid modeling system have to be modified. Physically, as shown in Eq. 6, the SSP nesting technique is equivalent to adding an interaction term $\left(-\frac{1}{\rho_o}\nabla_h\hat{p}\right)$ to the inner and outer model momentum equations, respectively. The interaction term depends on the density difference between the inner and outer models, with the linear coefficients β_i and β_o in Eqs. 8 and 9 determining the intensity of the interaction. In the case of $\beta_o = 1$, the outer model in the overlapping subregion is not constrained by the inner model. In the case of $\beta_i = 1$ the inner model is not constrained by the outer model except for the specification of the inner model boundary conditions based on the outer model results. As a result, the conventional one-way (C1W) nesting technique mentioned in Sect. 1 is equivalent to setting $\beta_o = \beta_i = 1$ in Eqs. 8 and 9.

For simplicity, we refer to the SSP nesting technique with $\beta_i = \beta_o = 0.5$ as the SSP two-way (SSP2W) nesting technique, and the one with $\beta_i = 0.5$, and $\beta_o = 1$ as the SSP one-way (SSP1W) nesting technique (Table 1). If the unsmoothed correction terms (i.e., the OSP method) are used in Eqs. 8 and 9, the nesting technique is referred to as the OSP nesting technique. We refer to the OSP nesting technique with $\beta_i = \beta_o = 0.5$ as the OSP two-way (OSP2W) nesting technique, and the one with $\beta_i = 0.5$ and $\beta_o = 1$ as the OSP one-way (OSP1W) nesting technique (Table 1). It can be seen that the main difference between the SSP1W (OSP1W) case and the C1W case is that the hydrostatic equation over the interior of the inner model domain in the SSP1W (OSP1W) case is constrained directly by the outer model density through the SSP(OSP) method, which is not true in the C1W case. (The OSP nesting technique was originally introduced in Sheng and Tang (2004); this method, however, leads to damping on the scale of the fine grid, and for this reason the SSP method described here is to be preferred—see Sect. Nested-grid modeling system of the Meso-American Barrier Reef System.)

It should be noted that the four versions of the new nesting technique discussed above (i.e., SSP2W, SSP1W, OSP2W and OSP1W cases, see Table 1) rely only on the exchange of the model density fields in the hydrostatic equations of the inner and outer models. As noted earlier, this is equivalent to modifying the momentum balance in the models. In particular, the model velocities, temperature and salinity fields are not exchanged directly between the two models, except for the use of the outer model results to specify the open boundary conditions for the inner model. Furthermore, the temperature and salinity equations for the component models are unchanged by the nesting procedure. It follows that both the SSP and OSP nesting techniques are adiabatic, and well-suited for tracer studies (Greatbatch et al. 2004).

The new two-way nesting technique can also be combined with the original version of the SSP method described in Eden et al. (2004); that is to correct for model systematic error and unsolved processes in multi-year simulations. Taking the inner model as an example, the hydrostatic equation of the inner model can be rewritten as

$$\frac{\partial p_{\text{inner}}}{\partial z} = -g\rho_{\text{inner}} - g(1-\beta_i)\langle\tilde{\rho}_i - \rho_{\text{inner}}\rangle \tag{10}$$

with the input density $\tilde{\rho}_i$ defined as

$$\tilde{\rho}_i = \alpha_i\hat{\rho}_{\text{outer}} + (1-\alpha_i)\rho_c \equiv \hat{\rho}_{\text{outer}} + (1-\alpha_i)(\rho_c - \hat{\rho}_{\text{outer}}), \tag{11}$$

where ρ_c is the climatological density calculated from climatological T/S fields, and α_i is the linear coefficient between 0 and 1. In the case of $\alpha_i = 0$, the input density $\tilde{\rho}_i$ is determined solely by the climatological density (ρ_c). In the case of $\alpha_i = 1$, $\tilde{\rho}_i$ is determined solely by the density calculated from outer model T/S fields after interpolation onto the fine grid ($\hat{\rho}_{\text{outer}}$), and climatological density does not affect the hydrostatic equation of the inner model.

Similarly, the hydrostatic equation of the outer model can be rewritten as

$$\frac{\partial p_{\text{outer}}}{\partial z} = -g\rho_{\text{outer}} - g(1-\beta_o)\langle\tilde{\rho}_o - \rho_{\text{outer}}\rangle \tag{12}$$

with the input density $\tilde{\rho}_o$ defined as

$$\begin{aligned}\tilde{\rho}_o &= \alpha_o\hat{\rho}_{\text{inner}} + (1-\alpha_o)\rho_c \\ &\equiv \hat{\rho}_{\text{inner}} + (1-\alpha_o)(\rho_c - \hat{\rho}_{\text{inner}}),\end{aligned} \tag{13}$$

Table 1 Specifications of the four versions of the new nesting technique based on the smoothed semi-prognostic method and the conventional one-way nesting technique

Index	Technique	Correction term	Nesting coefficients		γ^2 value	
			β_i	β_o	SS	MBRS
1	SSP2W	Smoothed	0.5	0.5	0.61	0.35
2	SSP1W	Smoothed	0.5	1.0	0.61	0.35
3	OSP2W	Unsmoothed	0.5	0.5	0.65	0.36
4	OSP1W	Unsmoothed	0.5	1.0	0.65	0.36
5	C1W		1.0	1.0	1.01	0.39

The γ^2 values used to assess the performance of these techniques using two independent nested-grid systems, one for the Scotian Shelf (SS) and the other for the Meso-American Barrier Reef System (MBRS)

where ρ_c is the climatological density, as before, and α_o is a linear coefficient between 0 and 1. In the case of $\alpha_o = 0$, the input density $\tilde{\rho}_o$ is determined solely by the climatological density (ρ_c). In the case of $\alpha_i = 0$, $\tilde{\rho}_o$ is determined solely by the density calculated from inner model T/S fields after interpolation onto the coarse grid ($\hat{\rho}_{\text{inner}}$), and climatological density does not affect the hydrostatic equation of the outer model.

In the application to the Scotian shelf described in Sect. 3, $\alpha_i = 1$ (that is, there is no correction made to the inner model using climatological data), but $\alpha_o = 0.5$ (i.e., climatological data is used to correct the outer model). For the application to the Meso-America Barrier Reef system described in Sect. 6, both α_i and α_o are set to 0.5. Outside the common subdomain of the inner and outer models, climatological data is used to adjust the outer model in both cases with $\alpha_o = 0$ and $\beta_o = 0.5$. It should be noted that, for both the nested systems, the OSP is used in the outer model outside the overlapping subregion.

Finally, we note that the nested-grid modeling systems described in Sects. 3 and 4 use the subgrid-scale mixing parameterization scheme of Smagorinsky (1963) for the horizontal eddy viscosity and diffusivity with the Prandtl number set to 0.1. Since the Smagorinsky scheme is resolution dependent, it has the desirable effect of leading to different levels of mixing in the inner and outer models. The vertical mixing scheme is the same in both the inner and outer models and uses Csanady's (1982) formula in the surface mixed layer and Large et al.'s (1994) formula in the interior of the ocean, with the Prandtl number set to 1.

3 Nested-grid modeling system of the Scotian Shelf

We first assess the performance of the new nesting technique using the nested-grid modeling system developed by Zhai et al. (2004) for the Scotian Shelf and slope (SSS) of the northwest Atlantic Ocean based on the primitive-equation, z-level ocean circulation model known as CANDIE (Sheng et al. 1998). The reader is referred to Sheng et al. (2001) and Zhai et al. (2004) for a detailed description of the model parameters and model setup. In this paper, we provide only a brief summary of the key elements of the system. We note that there is a demand for high resolution information on velocity and temperature and salinity variations on the SSS because of the growing offshore oil and gas industry, as well as aquaculture activities nearer shore, and it is for this reason that a nested modeling system for the region is of interest. An application of the nested modeling system to simulate the response of the SSS to Hurricane Juan in 2003 can be found in Sheng et al. (2005).

The nested system for the SSS comprises a fine-grid inner model and a coarse-grid outer model (Fig. 1). The fine-resolution inner model covers the area between 54°W and 66°W and between 39°N and 47°N, with a horizontal resolution of one-eleventh degree in longitude (about 7 km). The coarse-resolution outer model is the northwest Atlantic Ocean model developed by Sheng et al. (2001), which covers the area between 30°W and 76°W and between 35°N and 66°N, with a horizontal resolution of one-third degree in longitude. Both the inner and outer models use the ETOPO5 bathymetry (a gridded elevation/bathymetry compiled by the U.S. National Geophysical Data Center, National Oceanic and Atmospheric Administration) and have 31 unevenly spaced z levels, with the centers of each level located at 5, 16, 29, 44, 61, 80, 102, 128, 157, 191, 229, 273, 324, 383, 450, 527, 615, 717, 833, 967, 1,121, 1,297, 1,500, 1,733, 2,000, 2,307, 2,659, 3,063, 3,528, 4,061, and 4,673 m, respectively.

The model boundary conditions of the nested system are specified as follows. At the closed lateral boundaries of the inner and outer models, the normal flow, tangential stress and horizontal fluxes of T/S are set to zero (free-slip conditions). Along the model open boundaries, the normal flow and T/S fields are specified using the adaptive open boundary condition (Marchesiello et al. 2001), which first uses an explicit Orlanski radiation condition (Orlanski 1976) to determine whether the open boundary is passive (outward propagation) or active (inward propagation). If the open boundary is passive, the model prognostic variables are radiated outward to allow any perturbation generated inside the model domain to propagate outward through the open boundary as freely as possible. If the open boundary is active, the model prognostic variables at the open boundary are restored to input boundary fields. For the inner model, the input boundary fields are the simulated currents and T/S fields produced by the outer model after interpolation onto the fine grid, with a restoring time scale of 2 days. For the outer model, the input boundary fields are the monthly varying climatologies of T/S from Geshelin et al. (1999), the depth-mean normal flow is taken from the diagnostic calculation of Greatbatch et al. (1991), and the restoring time scale is 15 days. To eliminate the reflection of small-scale disturbances back into the model domain, a sponge layer is applied to the first ten grid points close to the open boundaries of the inner and outer models. The sponge layer is constructed by multiplying the horizontal eddy mixing coefficients determined from the Smagorinsky's scheme with an amplification factor that increases linearly from unity at the tenth grid point from the boundary to ten at the open boundary.

The nested system for the SSS is initialized with the January mean temperature and salinity from Geshelin et al. (1999) and forced by the monthly mean wind stress and surface heat flux from da Silva et al. (1994), the latter using the method of Barnier et al. (1995). The model sea surface salinity is restored to the monthly varying climatology with a time scale of 15 days. We conduct five numerical experiments by integrating the nested system for 2 years with the same model forcing and same sub-grid scale mixing parameterizations but using the five different nesting techniques listed in Table 1. Since the nested system is driven by monthly mean

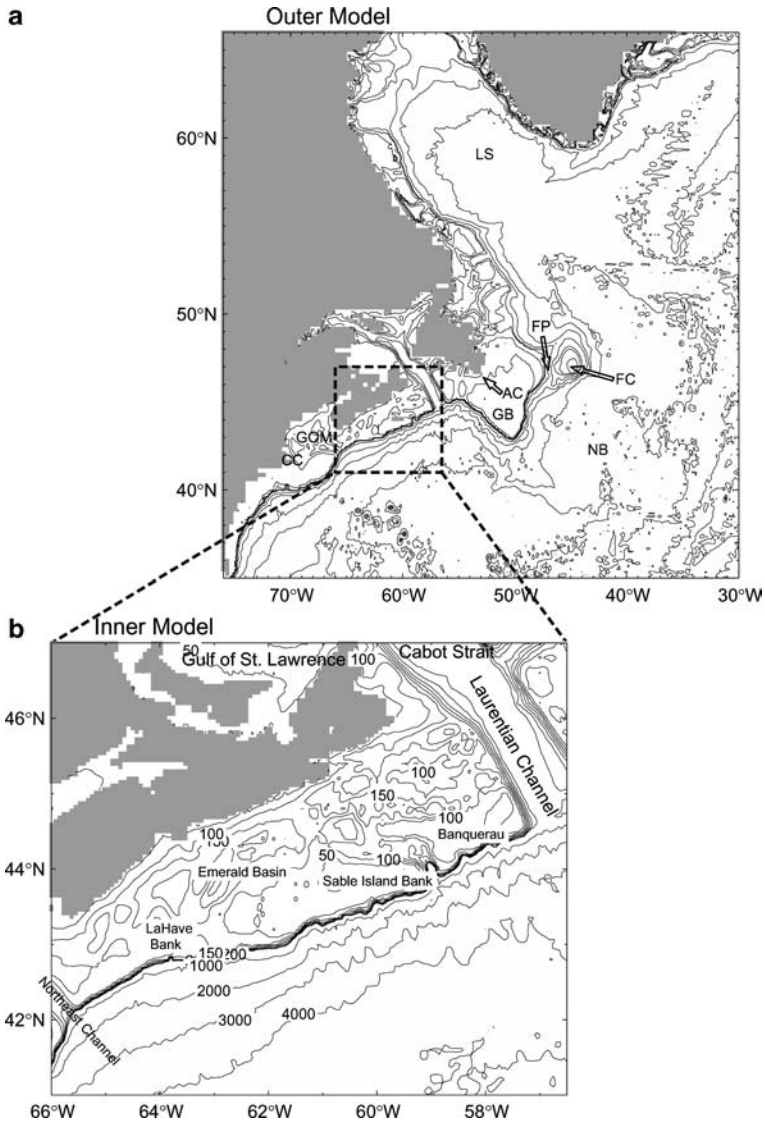

Fig. 1 Bathymetric features within **a** the outer model domain of the northwest Atlantic Ocean, and **b** the inner model domain of the Scotian Shelf and slope. Abbreviations are used for the Labrador Sea (*LS*), Flemish Cap (*FC*), Flemish Pass (*FP*), Avalon Channel (*AC*), Newfoundland Basin (*NB*), Grand Banks (*GB*), Gulf of Maine (*GOM*), and Cape Cod (*CC*)

forcings, the interaction rate between the inner and outer models is set to be once per day in this study. For the results shown here, the correction term in Eq. 8 is smoothed over 16 inner model grid points; that is, 112 km.

We first examine the simulated circulation and temperature over the northwest Atlantic Ocean produced by the outer model using the SSP2W nesting technique (the SSP2W case). The upper ocean circulation at day 690 (i.e., 30 November of the second model year, assuming 360 days for a model year) is shown in Fig. 2. In agreement with observations (Lazier and Wright 1993; Loder et al. 1998), there is a narrow southeastward jet along the shelf breaks of the Labrador and Newfoundland Shelves (the offshore branch of the Labrador Current). On reaching the northern flank of the Grand Banks, the offshore branch of the Labrador Current splits into three parts: a coastal branch that flows through the Avalon Channel, a middle branch that flows through Flemish Pass to the south, and an eastern branch that passes around the seaward flank of Flemish Cap (see Fig. 1 for the geographical locations). The middle branch and part of the eastern branch merge over the eastern flank of the Grand Banks and form a narrow equatorward jet along the shelf breaks of the Grand Banks and the Scotian Shelf. The outer model also produces reasonably well the general flow patterns of the Gulf Stream and North Atlantic Current offshore from the continental slopes of the Grand Banks and the Scotian Shelf. The large-scale circulation features produced by the outer model in the other four cases (i.e., the SSP1W, OSP2W, OSP1W and C1W cases, see the Appendix for the C1W case), as well as the single-domain model results presented in Sheng et al. (2001), are essentially the same as shown in Fig. 2. The main difference is that the outer model results using the two-way nesting technique (i.e., the SSP2W and OSP2W cases) have a slightly stronger recirculation over the slope water region due to the feedback from the inner model to the outer model in the SSP2W and OSP2W cases.

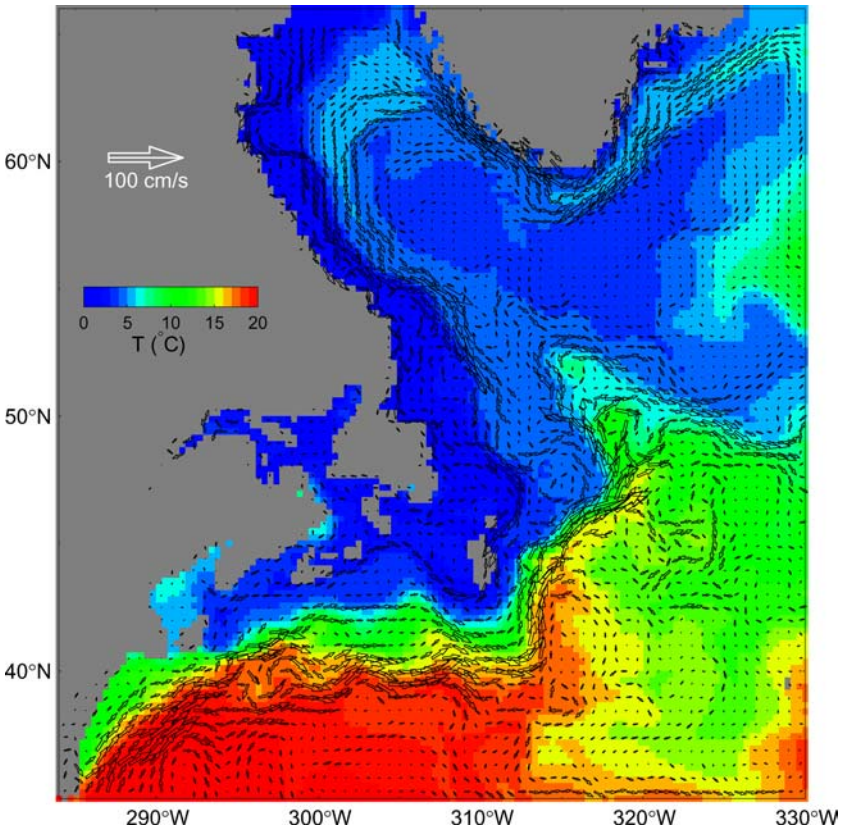

Fig. 2 Sub-surface (61 m) temperature and currents (*arrows*) at day 690 over the northwest Atlantic Ocean produced by the outer model in the SSP2W case. vectors are plotted at every second model grid point

We next examine the detailed circulation and temperature over the SSS where the inner and outer model grids overlap. The sub-surface (61 m) circulation at day 690 over this region produced by the inner model in the SSP2W case (Fig. 3b) is characterized by two southwestward jets on the Scotian Shelf, with an inshore jet (the Scotian Current) flowing along the coast and an offshore jet (the shelf-break jet) flowing along the outer shelf. Over the slope water region off the SS, there are two meso-scale recirculation gyres and an intense eastward flow as part of the Gulf Stream (Fig. 3b). This eastward jet splits into two branches at about 62°W, with the main branch flowing southeastward into the deep water and the weak branch flowing northeastward between the main branch and the shelf-break jet. The sub-surface temperature at day 690 produced by the inner model in the SSP2W case is characterized by cold intermediate waters of less than 5°C over the most of the Scotian Shelf, warm waters of greater than 20°C over the deep water, and sharp temperature gradients in the slope water region (Fig. 3b). The SSP2W nested inner model also reproduces a cold water tongue associated with the Labrador Current at the shelf break of the SS, which is one of the most important circulation features over the SSS region associated with the spreading of the Labrador Current from the Grand Banks to the Scotian Shelf (Smith et al. 1978; Loder et al. 1998).

The large-scale circulation features produced by the outer model in the SSP2W case (Fig. 3a) and those produced by the inner model in the SSP1W, OSP2W and OSP1W cases (Fig. 3c–e) compare reasonably well to those produced by the inner model in the SSP2W case (Fig. 3b). Main differences occur in the meso-scale features over the slope water region. The inner model in the SSP2W case generates more meso-scale features over the SSS, and a better defined cold water tongue at the shelf break of the SS than the outer model (Fig. 3a, b), which is expected since the inner model has a three times finer horizontal resolution than the outer model. In comparison with the inner model results in the SSP2W and SSP1W cases, the inner model results in the OSP2W and OSP1W cases have less-developed mesoscale circulation features in the slope water region, which is due mainly to the damping effect of the OSP method on the meso-scale eddy field discussed in Sect. 2.

Figure 3f shows the inner model results in the C1W case, in which the inner model is connected to the outer model only through the specification of the inner model boundary conditions taken from the outer model. As a result, the inner model can drift away from the outer model, as is evident in Fig. 3f. The inner model in the C1W case fails to generate the Scotian Current near the coast and the shelf-break jet associated with the Labrador current at the shelf break of the SS. The C1W nested inner model also fails to produce the widely recognized recirculation in the slope water region and overestimates significantly the sub-surface slope water temperature. Instead, the C1W nested inner model generates unrealistically large and broad northeastward flow over the slope water region, which differs significantly from the

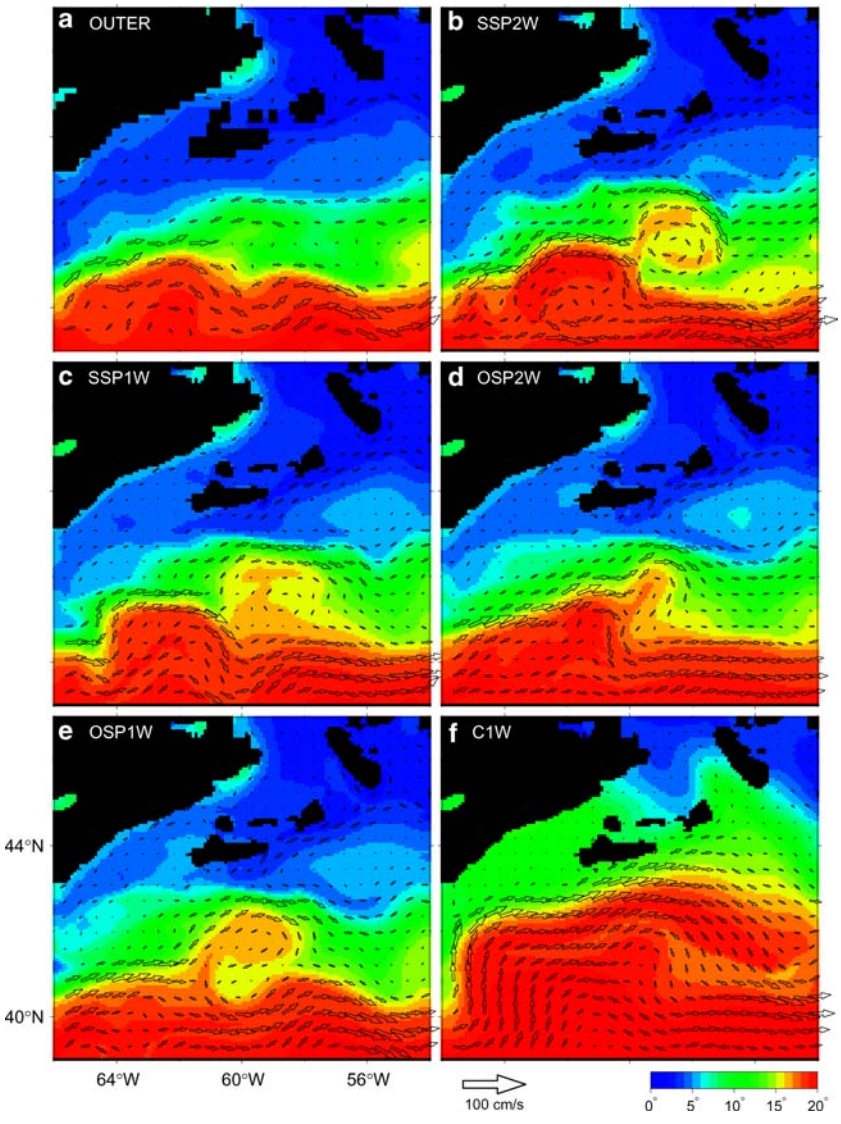

Fig. 3 Simulated sub-surface (61 m) temperature and currents (*arrows*) at day 690 over the Scotian Shelf and slope produced by **a** the outer model using the SSP2W nesting technique and the inner model using **b** the SSP2W, **c** SSP1W, **d** OSP2W, **e** OSP1W, and **f** C1W nesting techniques. Velocity vectors are plotted at every fourth model grid point for the inner model and every second model grid point for the outer model over the inner model domain

inner model results in other four cases (Fig. 3b–e). The failure of the C1W case highlights one of the advantages of semi-prognostic nesting; namely, to prevent unrealistic drift of the inner model. (The unrealistic drift of the inner model in the C1W case is discussed further in the Appendix.)

The second year model results in the five cases are used to calculate the annual mean near-surface currents over the SSS region at 16 m depth (Fig. 4). Figure 4b, for the inner model in the SSP2W case, shows the annual mean southwestward Scotian Current, the narrow shelf break jet, and the narrow jet over the slope water offshore from the SS that first flows northeastward over the slope water region off the southwestern SS and then turns eastward to the deep water off the southeastern SS. Further south of the slope water region, there is a strong and broad eastward flow as part of the Gulf Stream. The annual mean circulation produced by the SSP2W nested inner model is consistent with our current knowledge of time-mean circulation in the SSS (Lazier and Wright 1993; Loder et al. 1998; Smith et al. 1978; Sheng and Thompson 1996). The annual mean near-surface currents produced by the inner model in the SSP1W, OSP2W and OSP1W cases (Fig. 4c–e) compare reasonably well with the annual mean near-surface currents produced by the SSP2W nested inner model results (Fig. 4b). By contrast, the annual mean near-surface currents produced by the inner model using the C1W nesting technique (Fig. 4f) differ significantly from the inner model results in the other four cases shown in Fig. 4b–e.

To further demonstrate the advantage of the new two-way nesting technique based on the smoothed semi-prognostic method, we compare the annual mean near-surface (16 m) currents produced by the nested system with the time mean currents in the 1990s inferred by Fratantoni (2001) from the observed trajectories of near-surface drifters over the SSS. The annual mean currents produced the inner model in the SSP2W and SSP1W cases (Fig. 4b,c) reproduce reasonably well the

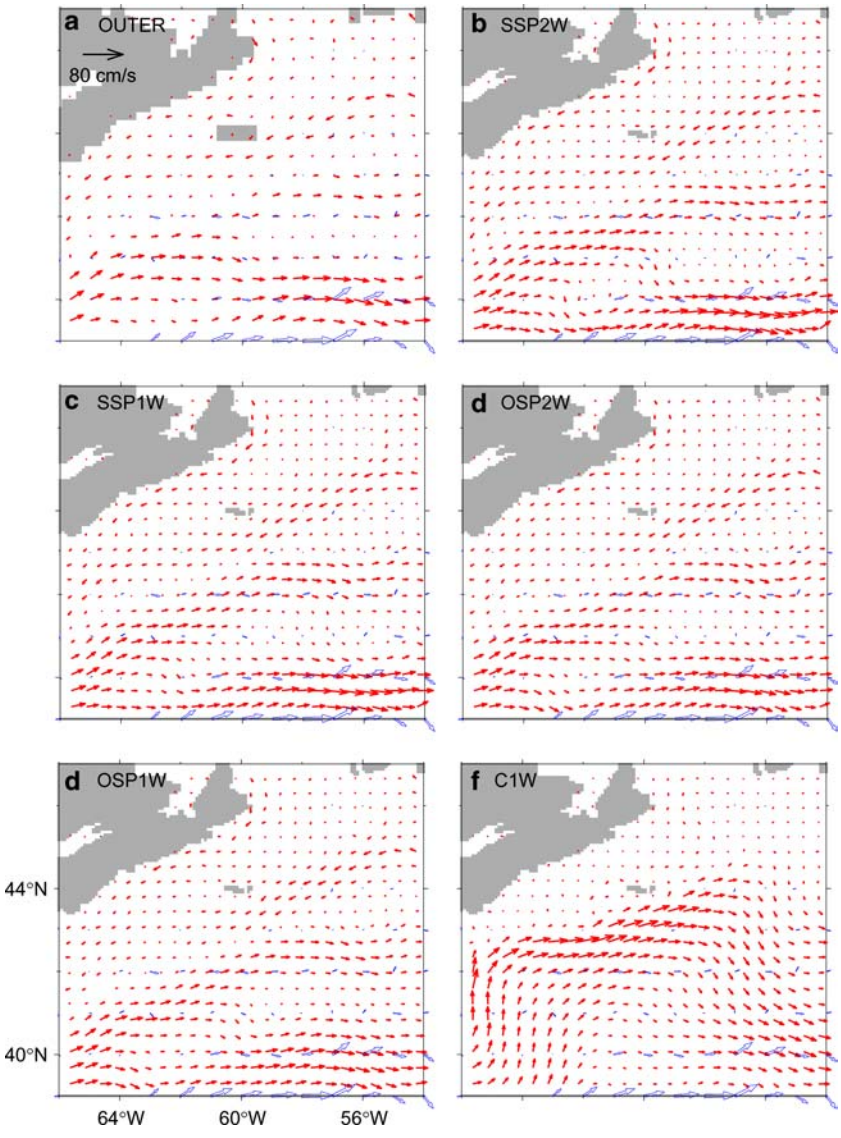

Fig. 4 Comparison of simulated (*solid red arrows*) and observed (*open black arrows*) near-surface currents over the Scotian Shelf and slope (SSP). The observed currents are the gridded time-mean near-surface currents during the 1990s inferred from trajectories of 15 m-drogued satellite-tracked drifters by Fratantoni (2001) on a 1° grid. The simulated currents are the annual mean currents at 16 m calculated from the second year model results generated by **a** the outer model using the SSP2W nesting technique and those by the inner model using **b** the SSP2W, **c** SSP1W, **d** OSP2W, **e** OSP1W, and **f** C1W nesting techniques. Velocity vectors are plotted at every fourth model grid point for the inner model and every second model grid point for the outer model

large-scale features of the observed currents. The SSP2W outer model results (Fig. 4a) are also in qualitative agreement with the observed currents. To quantify the misfit between the observed and model-calculated near-surface currents, we use a value of γ^2 defined as

$$\gamma^2 = \frac{\sum_k^N [(u_k{}^o - u_k{}^s)^2 + (v_k{}^o - v_k{}^s)^2]}{\sum_k^N [(u_k{}^o)^2 + (v_k{}^o)^2]}, \qquad (14)$$

where (u_k^o, v_k^o) are the horizontal components of the observed near-surface currents at the kth location estimated by Fratantoni (2001), (u_k^s, v_k^s) are the horizontal components of the simulated near-surface currents at the same location as the observations, and N is the total number of locations where observed estimates are available. Clearly, the smaller γ^2, the better the model results fit the observations.

For the nested-grid system of the SS using the SSP2W nesting technique, the γ^2 value is about 0.73 for the outer model and 0.61 for the inner model (Fig. 5a,b and Table 1), indicating that the inner model performs better than the outer model in reproducing Fratantoni's observed currents. The inner model in the OSP2W and OSP1W cases also reproduces reasonably well the time-mean observed near-surface currents over the SSS (Figs. 4d,e and 5d,e), with γ^2 values of about 0.65 in both cases (Table 1), which are comparable to, and slightly larger than, the γ-values in the SSP2W and SSP1W cases, indicating that the nested-grid system of the SS using the original semi-prognostic (OSP) nesting technique performs slightly worse than that using the smoothed semi-prognostic (SSP) nesting technique in reproducing Fratantoni's data. The inner model results in the C1W case agree the least well with Fratantoni's time-mean observed near-surface currents (Fig. 5f), with the γ^2 value of about 1.01, which is about 60% larger than that of the inner model results in other four cases (Table 1).

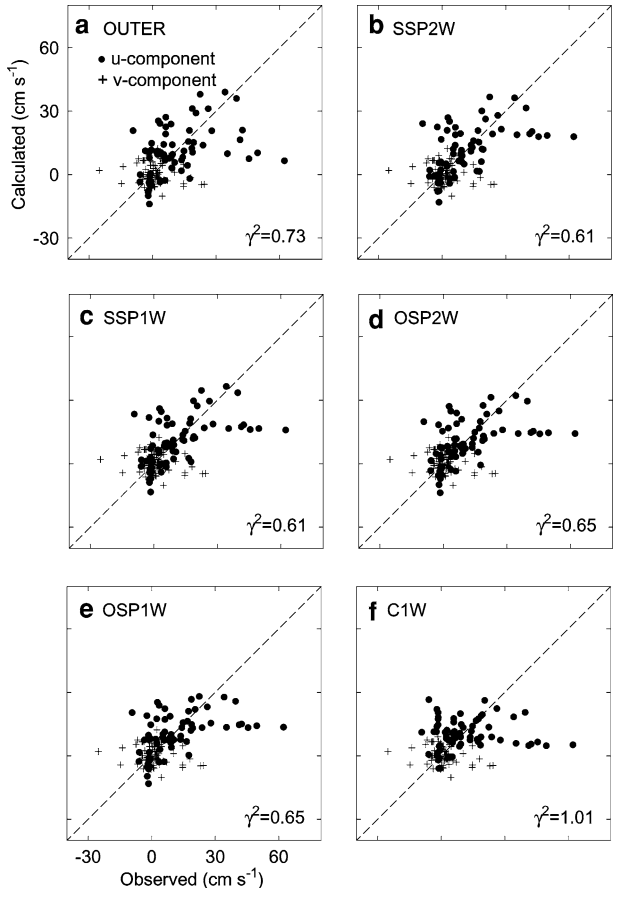

Fig. 5 Scatterplots of the observed and simulated time-mean near-surface currents over the SSP. The observed currents are the decadal-mean near-surface currents during the 1990s inferred from trajectories of 15 m-drogued satellite-tracked drifters (Fratantoni 2001). The simulated time-mean currents are those at the same locations as the observations interpolated from the annual mean circulation calculated from the second-year model simulations at 16 m produced by **a** the outer model using the SSP2W nesting technique by the inner model using **b** the SSP2W, **c** SSP1W, **d** OSP2W, **e** OSP1W, and **f** C1W nesting techniques. *Dashed line* represents perfect fit for reference

4 Nested-grid modeling system of the Meso-American Barrier Reef System

We next assess the performance of the four versions of the new nesting technique using the nested-grid modeling system developed by Sheng and Tang (2004) for the Meso-American Barrier Reef System (MBRS) over the northwestern Caribbean Sea. The reader is referred to Sheng and Tang (2004) for a detailed description of the model parameters and setup of the system. Only a brief summary of the system is provided here. We note that there is an increasing demand for a nested modeling system for the MBRS since this area serves as an important breeding and feeding ground for marine mammals, reptiles, fish and invertebrates, many of which are of commercial importance. The MBRS also contributes significantly to the protection of coastal landscapes and the maintenance of coastal water quality. The unique marine ecosystems in the MBRS have been significantly affected by natural and anthropogenic influences such as eutrophication of coastal waters, excessive terrestrial runoff and sedimentation from deforestation. Reliable simulations of the ocean circulation in the MBRS using a nested-grid model are required for an effective management of the coastal and marine ecosystems in the area.

The nested system for the MBRS comprises the fine-grid inner model and the coarse-grid outer model shown in Fig. 6. The inner model domain covers the area between 79°W and 89°W and between 15.5°N and 21.5°N, with a horizontal resolution of about 6 km. The outer model is the western Caribbean Sea model (Sheng and Tang 2003), which covers the area between 72°W and 90°W and between 8°N and 24°N, with a horizontal resolution of about 19 km. The nested-grid system of the MBRS uses the same vertical discretization with 31 z-levels, the same sub-grid mixing parameterizations and the same formulation for the open boundary conditions as the nested system of the Scotian Shelf, except that the depth-mean flow along the outer model open boundaries of the MBRS nested system is the depth-mean flow taken from a (1/3)° FLAME model simulation of the North Atlantic Ocean (FLAME stands for the Family of Linked Atlantic Model Experiments, Dengg et al. 1999). The nested system of the MBRS is initialized with January mean climatologies of temperature and salinity and

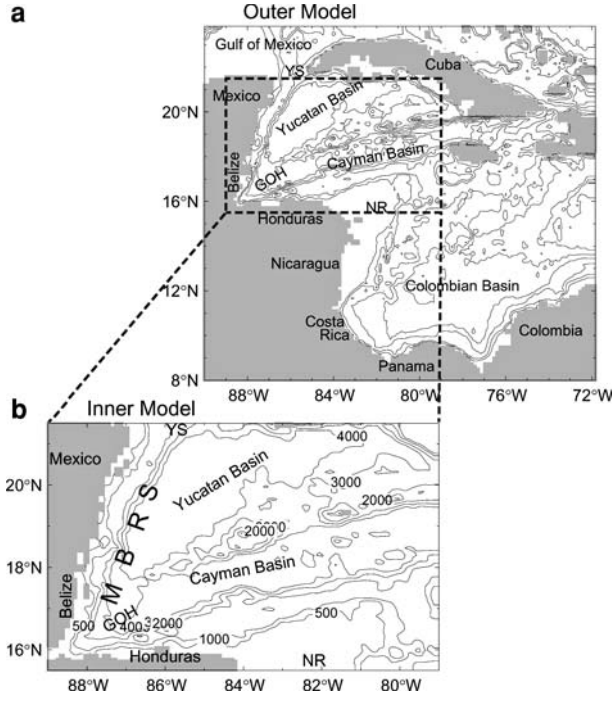

Fig. 6 Bathymetric features within **a** the outer model domain of the western Caribbean Sea, and **b** the inner model domain of the Meso-American Barrier Reef System (MBRS). Abbreviations are used for Yucatan Strait (*YS*), Gulf of Honduras (*GOH*) and Nicaragua Rise (*NR*)

forced by the monthly mean wind stress and surface heat flux taken from da Silva et al. (1994), with the model sea surface salinity restored to the monthly mean climatology, as before. Also, as before, the inner and outer models interact once per day, and the smoothing scale in Eq. 8 corresponds to 16 model inner model grid points (that is about 112 km). Similarly, we conduct five numerical experiments by integrating the nested system of the MBRS for two years using the five different nesting techniques listed in Table 1.

The sub-surface (61 m) circulation at day 720 (end of December of the second model year) produced by the SSP2W nested outer model is dominated by the Caribbean Current flowing from the northern Colombian Basin to the western Yucatan Basin, with two cyclonic recirculations in the southwestern Caribbean Sea known as the Panama-Colombia Gyre (Fig. 7). The Caribbean Current is relatively broad and almost westward in the central and eastern Colombian Basin. This current bifurcates before reaching Nicaragua Rise, with one small branch veering southwestward to form the Panama-Colombia Gyre. The main branch of the current turns northwestward and flows onto the northwest Caribbean Sea to form an offshore flow running westward off the northern coast of Honduras. This offshore flow turns northward as it approaches the Gulf of Honduras and then runs northward along the east coast of Belize and Mexico. The simulated sub-surface temperature at day 690 produced by the SSP2W outer model (Fig. 7) is characterized by a strip of warm subsurface water of about 27°C along the pathway of the Caribbean Current over the northern Colombian Basin and southwestern Cayman Basin, with two pools of cold waters associated with the cyclonic Panama-Colombia Gyre over the southwestern Colombian Basin. The SSP2W nested outer model results are essentially same as the single-domain model results of the western Caribbean Sea discussed in Sheng and Tang (2003) and in general agreement with our current knowledge of general circulation in the region (Mooers and Maul 1998; Johns et al. 2002).

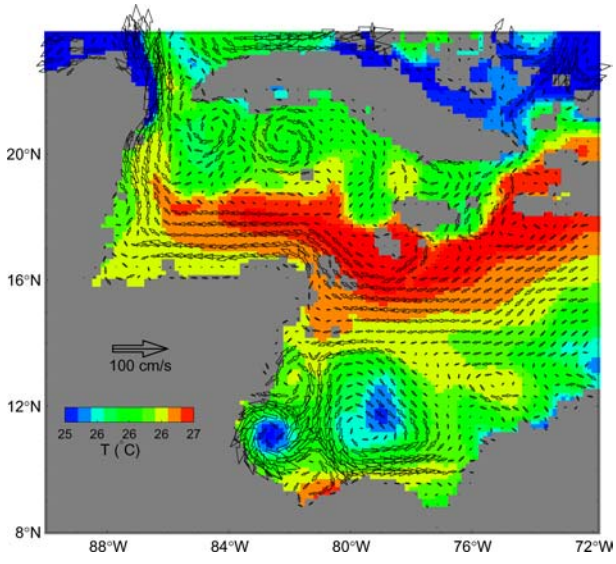

Fig. 7 Simulated sub-surface (61 m) temperature and currents (*arrows*) at day 720 over the western Caribbean Sea produced by the SSP2W nested outer model. Velocity vectors are plotted at every second model grid point

The outer model results in the other four cases (i.e., SSP1W, OSP2W, OSP1W, and C1W) have very similar large-scale features as those produced by the outer model in the SSP2W case. The main differences occur in the meso-scale features over the northwestern Caribbean Sea. The outer model in the SSP2W and OPS2W cases produces more meso-scale features over this region than those in the SSP1W, OSP1W and C1W cases, which is due to the feedback from the inner model to the outer model.

Figure 8 shows the detailed sub-surface (61 m) currents and temperature at day 720 produced by the nested system in the five cases over the northwestern Caribbean where the outer and inner model grids overlap. The subsurface circulation at this time produced by the SSP2W nested inner model (Fig. 8b) is dominated by a narrow and intense throughflow as part of the Caribbean Current. The intense throughflow enters the northwestern Caribbean Sea along the outer flank of Nicaragua Rise and then flows westward about 200 to 300 km off the northern coast of Honduras. The throughflow veers anticyclonically to flow northward along the eastern coast of Belize and Mexico after passing the Gulf of Honduras. The simulated sub-surface temperature at day 720 produced by the SSP2W nested inner model is characterized by a narrow strip of relatively warm water that is advected by the Caribbean Current from the outer flank of Nicaragua Rise to the western part of Cayman and Yucatan Basins. Figure 8b also demonstrates several pools of relatively cold sub-surface water associated with local upwelling near the northern coast of Honduras and east coast of Yucatan Peninsula.

The SSP2W nested inner model generates more intense throughflow over the northwestern Caribbean with more meso-scale features (Fig. 8b) than the SSP2W nested outer model (Fig. 8a), due to the finer horizontal resolution used in the inner model. The inner model results in the SSP1W case compare very well to those in the SSP2W case (Fig. 8b, c), indicating that the feedback from the inner model to the outer model plays a secondary role in affecting the inner model results. In comparison, the inner model results in the OSP2W and OSP1W cases (Fig. 8d, e) have large-scale features consistent with those in the SSP2W and SSP1W cases, but with much less meso-scale features in the former two cases due to the smoothing effect of the the OSP discussed in Sect. 2. Of particular note, are the much more pronounced cold pools near the northern coast of Honduras in the SSP compared to the OSP cases.

In comparison with the model results shown in Fig. 8b–e, the sub-surface circulation at day 920 produced by the inner model in the C1W case (Fig. 8f)

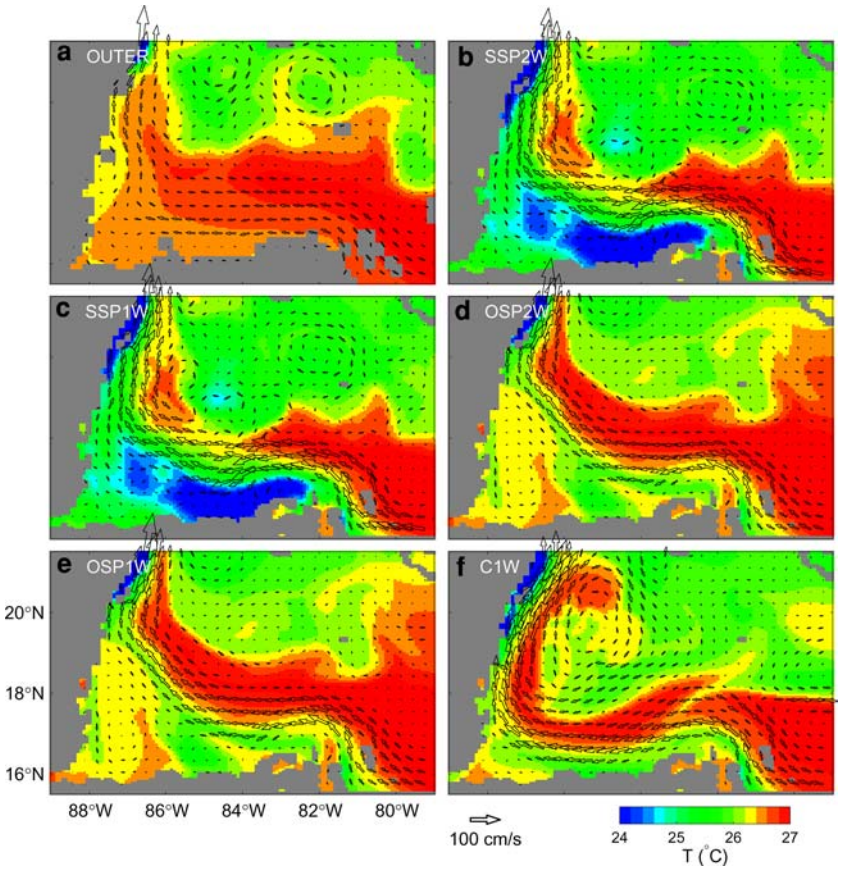

Fig. 8 Simulated sub-surface (61 m) temperature and currents (*arrows*) at day 720 over the northwest Caribbean Sea produced by the outer model using the SSP2W nesting technique and those by **a** the inner model using **b** the SSP2W, **c** SSP1W, **d** OSP2W, **e** OSP1W, and **f** C1W nesting techniques. Velocity vectors are plotted at every fifth model grid point for the inner model and every second model grid point for the outer model

differs significantly from the inner model results using the four variants of the new nesting technique. The simulated sub-surface throughflow over the northwest Caribbean Sea produced by the C1W nested inner model is too close the north coast of Honduras. The large-scale anticyclonic gyre over the western Yucatan Basin produced by the C1W nested inner model also differs significantly from the inner model results in other four cases.

We also calculate the annual mean near-surface currents at 16 m from the second year inner model simulation (Fig. 9) and compare them with Fratantoni's decadal mean near-surface currents in the northwestern Caribbean Sea. The time-mean near-surface currents produced by the inner model in the SSP2W, SSP1W and OSP2W and OSP1W cases (Fig. 8b–e) are characterized by a persistent throughflow that enters the Cayman Basin from the outer flank of Nicaragua Rise to form a narrow westward flow off the northern coast of Honduras. This westward jet turns anticyclonically to run northward along the eastern coast of Belize and Mexico after passing the Gulf of Honduras, and compares well with the observed near-surface currents in the region. The γ^2 values are about 0.35 for the inner model results in the SSP2W and SSP1W cases and 0.36 in the OSP2W and OPS1W cases (Table 1 and Fig. 10b–c). Therefore, all the four types of the new nesting technique perform equally well in reproducing Fratantoni's time-mean near-surface currents in the northwest Caribbean Sea.

The time-mean sub-surface circulation produced by the C1W nested inner model (Fig. 9f) has large-scale features that compare qualitatively to the observed currents, with the simulated throughflow spreading too much to the Gulf of Honduras and deep water of the central Yucatan Basin. The γ^2 value in the C1W case is about 0.39 (Fig. 10f), which is slightly larger than the values in other four cases. The outer model in the SSP2W case fits the data the least well (Figs. 9a, 10a) with Fratantoni's data, with the γ^2 value of about 0.43. Due mainly to the coarse resolution, the outer model underestimates the observed currents significantly, with the simulated throughflow too broad in comparison with the inner model results in other four cases.

5 Summary and conclusions

A new two-way nesting technique based on the SSP method (Eden et al. 2004) has been developed for a nested-grid ocean circulation modeling system. The SSP method is a modification of the OSP method introduced by Sheng et al. (2001). The original application of both the SSP and OSP methods was to adjust a model to correct for systematic error in multi-year simulations (see Greatbatch et al. 2004 for a comprehensive review). In this paper, we have demonstrated that both the SSP and OSP methods can be used to exchange information between the sub-components of a nested-grid modeling

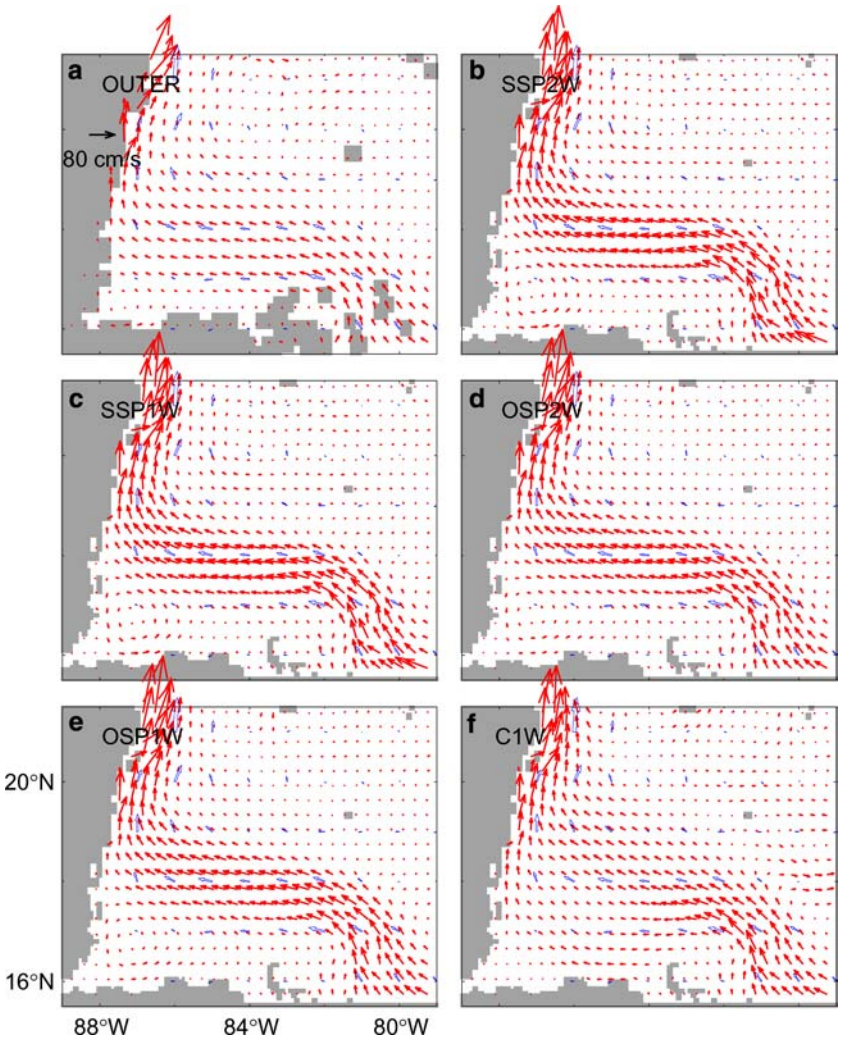

Fig. 9 Comparison of simulated (*solid arrows*) and observed (*open arrows*) near-surface currents over the northwestern Caribbean Sea. The observed currents are the gridded time-mean near-surface currents during the 1990s inferred from trajectories of 15 m-drogued satellite-tracked drifters by Fratantoni (2001) on a 1° grid. The modeled currents are the annual mean currents at 16 m computed from the second-year model results generated by **a** the outer model using the SSP2W nesting technique and those by the inner model using **b** the SSP2W, **c** SSP1W, **d** OSP2W, **e** OSP1W, and **f** C1W nesting techniques. Velocity vectors are plotted at every fifth model grid point for the inner model and every second model grid point for the outer model

system by introducing an interaction term in the model horizontal momentum equations. The new nesting technique is very easy and straightforward to implement in the model code since only the hydrostatic equations in the subcomponents of the nested-grid modeling system need to be modified. The new nesting technique can also easily be applied to a multiple nested-grid modeling system; that is a system with several fine-resolution inner models embedded inside a coarse-grid outer model, and one or more finer-resolution local models embedded inside each inner model. The main advantage of semi-prognostic nesting is that because the outer model is used to constrain the inner model within the interior of the inner model domain, unrealistic drift of the inner model is effectively prevented. (The tendency for the inner model to drift unrealistically is discussed in Appendix.)

Depending on the use of the SSP or OSP methods and one-way or two-way nesting, four different types of the new nesting technique were introduced in this paper. They are the SSP two-way (SSP2W), SSP one-way (SSP1W), OSP two-way (OSP2W), and OSP one-way (OSP1W) nesting techniques. The common features of these four types of the new technique are that (1) the inner model open boundary conditions are specified based on the outer model results; and (2) the outer model results are used to constrain the inner model momentum equations over the interior of the inner model domain based on the semi-prognostic method. The main difference between the SSP and OSP nesting techniques is that the SSP nesting technique uses a spatially smoothed (large-scale) interaction term, while the OSP nesting technique uses an unsmoothed interaction term. Smoothing of the interaction term in the SSP case releases the fine scales associated with the inner model grid, ensuring that the maximum benefit is obtained from the higher resolution of the inner model, while at the same time still using the outer model to constrain the inner model on large spatial scales (large compared to the smoothing scale). The main difference between the one-way and two-way nesting using the SSP or OSP method is that the inner model is used to adjust the outer model over the overlapping subregion in two-way nesting, while there is no feedback from the inner model to the outer model in the one-way nesting. By comparison, the conventional one-way (C1W) nesting

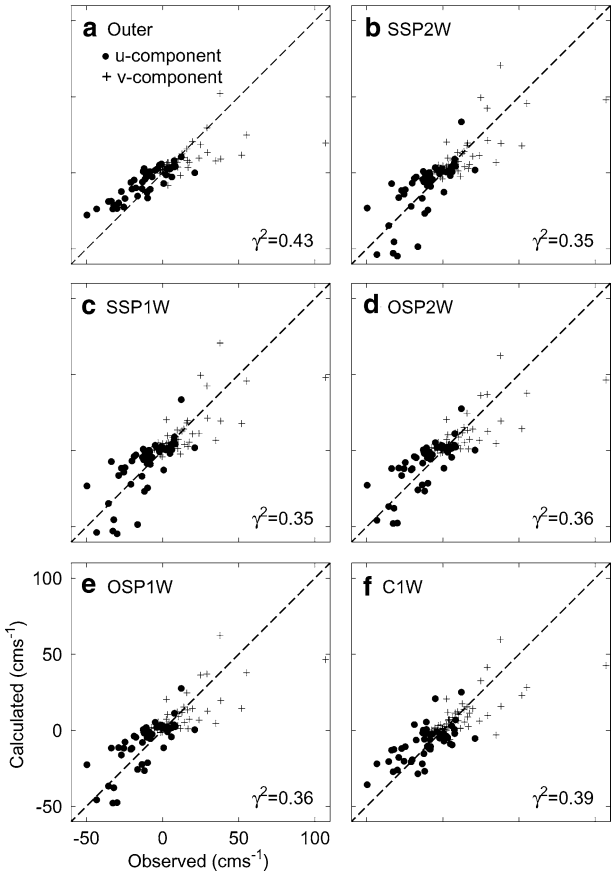

Fig. 10 Scatterplots of observed and model-computed time-mean near-surface currents in the northwest Caribbean Sea. The observed currents are the decadal-mean near-surface currents during the 1990s inferred from trajectories of 15 m-drogued satellite-tracked drifters by Fratantoni (2001). The model-computed currents are those at the same locations as the observations interpolated from the second-year model simulations at 16 m by **a** the outer model using the SSP2W nesting technique and those by the inner model using **b** the SSP2W, **c** SSP1W, **d** OSP2W, **e** OSP1W, and **f** C1W nesting techniques. *Dashed line* represents perfect fit for reference

technique connects the inner model to the outer model only through the specification of the inner model boundary conditions taken from the outer model. The C1W nesting technique does not allow the outer model to constrain directly the inner model results over the interior of the inner model domain, neither does it allow any feedback from the inner model to the outer model.

The performance of the four versions of the new nesting technique, as well as C1W nesting, was assessed using two independent nested-grid ocean circulation modeling systems, with one for the Meso-American Barrier Reef System (MBRS) northwest Caribbean Sea and the other for the Scotian Shelf of the northwest Atlantic Ocean. Both nested systems comprise a fine-resolution inner model and a coarse-resolution outer model. Comparison of the instantaneous circulation and temperature field produced by the inner models demonstrates that the SSP2W nesting technique performs better than the SSP1W, OSP2W and OSP1W nesting techniques and much better than the C1W nesting technique. We also assessed the performance of the new nesting technique by comparing the annual mean near-surface currents produced by the five different nesting methods with the decadal-mean near-surface currents estimated by Fratantoni (2001) from the observed trajectories of sub-surface drifters in the 1990s. We found that the SSP2W and SSP1W nesting techniques perform equally well and both methods perform significantly better than the C1W nesting technique in reproducing time-mean near-surface circulation in the MBRS of the northwestern Caribbean Sea and Scotian Shelf of the northwestern Atlantic Ocean. This indicates the importance of adjusting the interior of the inner model using outer model fields (a feature of semi-prognostic nesting), while the feedback from the inner model to the outer model plays a less important role in affecting the annual mean circulation in the two study regions.

Acknowledgements We wish to thank Carsten Eden for his initial suggestion of developing a two-way nesting technique based on the smoothed semi-prognostic method. We also thank Chris Mooers, Alan Davies, Jiuxing Xing, Leo Oey and two anonymous reviewers for their useful comments. We thank David Fratantoni for providing the near-surface currents determined from the 10 m-drogued satellite-tracked drifters in the North Atlantic. This work has been supported by funding from CFCAS and NSERC. R.J.G. and J.S. are also supported by NSERC, MARTEC (a Halifax based company), and the Meteorological Service of Canada (MSC) through the NSERC/MARTEC/MSC Industrial Research Chair in "Regional Ocean Modeling and Prediction".

6 Appendix

7 Drift of the inner model under C1W nesting

Unrealistic drift of the inner model occurs in the conventional one-way (C1W) nesting cases discussed in Sects. 3 and 4. Here we investigate the causes of this drift by describing two experiments (Exp A1 and A2) in which the inner and outer models have the same resolution. The model setup and parameters are the same as the C1W case discussed in Sect. 3 (see Figs. 3f, 4f), except that the inner model horizontal resolution is set to about 25 km, which is very close to the horizontal resolution (one third degree in longitude) of the outer model on the SSS.

In Exp A1, the inner model is fully prognostic (that is, $\alpha_i = 1$ and $\beta_i = 0$ in Eqs. 10 and 11), exactly as in the previous C1W case, with the normal flow and T/S fields along its open boundaries specified in terms of outer model variables (see Sect. 3 for more discussion of model open boundary conditions). In the Exp A2, the OSP is used to constrain the inner model using climatological data (by setting $\alpha_i = 0$ and $\beta_i = 0.5$ in Eqs. 10 and 11 and without using the smoothing operator), and

all other model parameters are the same as those in Exp A1. Use of the OSP in this case ensures that the inner model is run in exactly the same way as the outer model (which is also constrained using the OSP with climatological data as input) and means that any differences between the inner and outer models in Exp A2 can only be because of the open boundary formulation applied to the inner model.

Figure 11a and b shows the instantaneous temperature and circulation at day 690 (30 November of the second model year) at depths of 16 m (near-surface) and 61 m (sub-surface) produced by the outer model in these experiments. The large-scale circulation features compare well with those produced by the same outer model but using the SSP two-way nesting technique (Fig. 3a). Differences occur mainly in the mesoscale circulation features and can be explained by the fact that there is no feedback from the inner to the outer model in Exps A1 and A2.

The inner model in Exps A1 (Fig. 11c, d) and A2 (Fig. 11e, f) has similar circulation features as the outer model (Fig. 11a, b), but there are also differences, especially in the mesoscale circulation features. This is true even in Exp A2, which is identical to the outer model apart from the use of the open boundary formulation used to connect the inner model to the outer model. Based on these experiments we conclude that the unrealistic drift of the inner model evident from Fig. 3f is primarily a consequence of the much higher horizontal resolution of the inner compared to the outer model in that case, although some influence from the open boundary formulation is also likely. Finally, we note that implicit in the higher horizontal resolution of the inner model is a reduction in the horizontal mixing on the inner compared to the outer model grid (due to the use of the Smagorinsky scheme), and enhanced resolution of the irregular bottom topography and coastline on the shelf. Both these factors that are

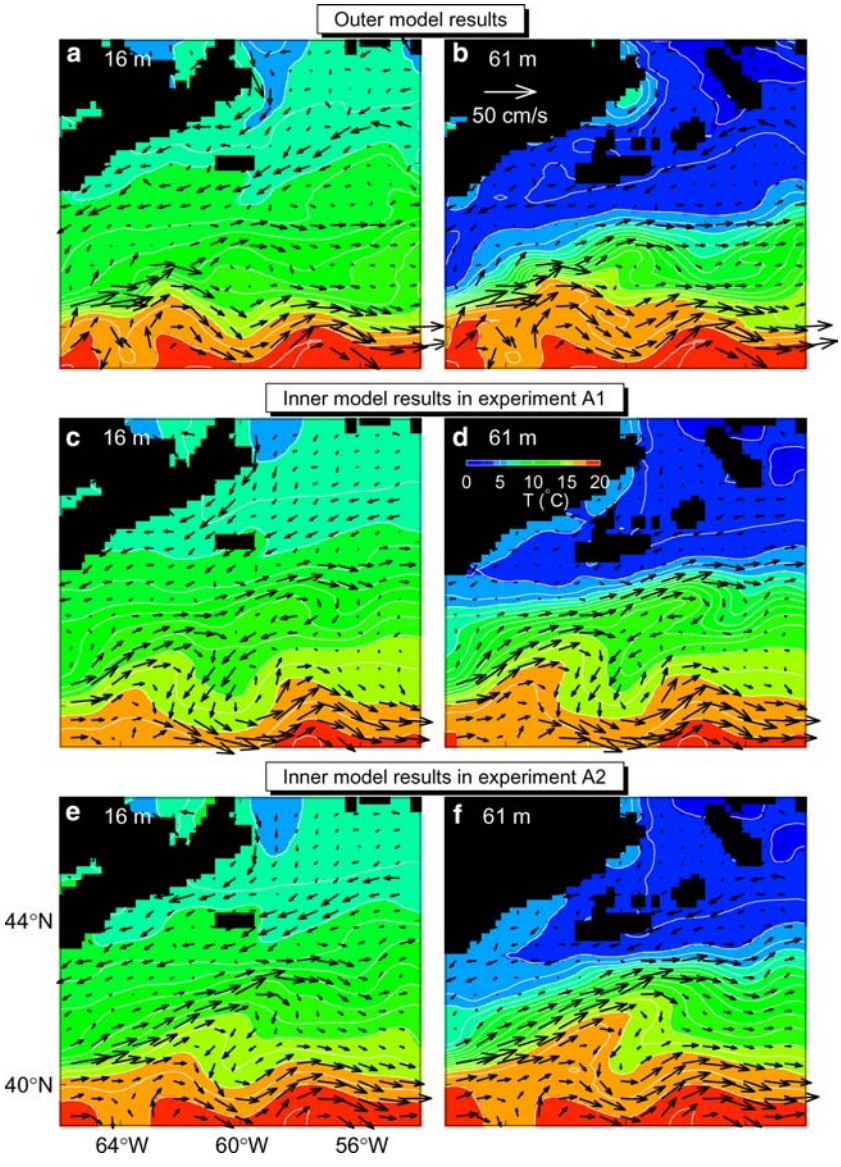

Fig. 11 Temperature and currents (*arrows*) at day 690 over the inner model domain produced by the nested modeling system for the Scotian Shelf, using the conventional one-way (C1W) nesting technique. The horizontal resolution of the inner and outer models on the Scotian Shelf and slope are essentially the same in the two experiments. *Top panels* show the outer model results at depths of **a** 16 m and **b** 61 m. The *middle* and *lower panels* show the inner model results from Exps A1 and A2, respectively, at depths of (**c**, **e**) 16 m and (**d**, **f**) 61 m. (See text for details)

inherent, and unavoidable, aspects of anynested modeling system.

References

Barnier B, Siefridt L, Marchesiello P (1995) Thermal forcing for a global ocean circulation model using a three-year climatology for ECMWF analyses. J Mar Syst 6:363–380

Bell MJ, Martin MJ, Nichols NK (2004) Assimilation of data into an ocean model with systematic errors near the equator. Q J R Meterol Soc 130:873–893

Csanady GT (1982) Circulation in the coastal Ocean. Reidel, Dordrecht, pp 279

Eden C, Greatbatch RJ, Böning CW (2004) Adiabatically correcting an eddy-permitting model of the North Atlantic using large-scale hydrographic data. J Phys Oceanogr 34:701–719

Dengg J, Boening CW, Ernst U, Redler R, Beckmann A (1999) Effects of an improved model representation of overflow water on the subpolar North Atlantic. Int WOCE Newslett 37:10–15

Durran DR (1999) Numerical methods for wave equations in geophysical fluid dynamics. Springer, Berlin Heidelberg New York, pp 465

Fox AD, Maskell SJ (1995) Two-way interactive nesting of primitive equation ocean models with topography. J Phys Oceanogr 25: 2977–2996

Fratantoni DF (2001) North Atlantic surface circulation during the 1990's observed with satellite-tracked drifters. J Geophys Res 106:22067–22093

Geshelin Y, Sheng J, Greatbatch RJ (1999) Monthly mean climatologies of temperature and salinity in the western North Atlantic. Can Data Rep Hydrogr Ocean Sci 153:62

Ginis I, Richardson A, Rothstein L (1998) Design of a multiply nested primitive equation ocean model. Mon Wea Rev 126: 1054–1079

Greatbatch RJ, Fanning AF, Goulding AD, Levitus S (1991) A diagnosis of interpentadal circulation changes in the North Atlantic. J Geophys Res 96:22009-22023

Greatbatch RJ, Sheng J, Eden C, Tang L, Zhai X, Zhao J (2004) The semi-prognostic method. Cont Shelf Res 24:2149–2165

Griffies SM, Boning C, Bryan FO, Chassignet EP, Gerdes R, Hasumi H, Hirst A, Treguier A-M, Webb D (2000), Developments in ocean climate modelling. Ocean Model 2:123–192

Kurihara Y, Tripoli GJ, Bender MA (1979) Design of a movable nested-mesh primitive equation model. Mon Wea Rev 107: 239–249

Haidvogel DB, Wilkin JL, Young RE (1991) A semi-spectral primitive equation regional ocean circulation model using vertical sigma and orthogonal curvilinear horizontal coordinates. J Comput Phys 94:151–185

Johns WE, Townsend TL, Fratantoni DM, Wilson WD (2002) On the Atlantic inflow to the Caribbean Sea. Deep Sea Res I 49:211–243

Jones JE (2002) Coastal and shelf-sea modelling in the European context. Oceanogr Mar Biol Annu Rev 40:37–141

Large WG, McWilliams JC, Doney SC (1994) Oceanic vertical mixing: a review and a model with a nonlocal boundary layer parameterization. Rev Geophys 32:363–403

Lazier JRN, Wright DG (1993) Annual velocity variations in the Labrador Current. J Phys Oceanogr 23:659–679

Le Provost C, Genco ML, Lyard F, Vincent P, Canceil P (1994): Spectroscopy of the world tides from a finite element hydrodynamic ocean tide model. J Geophys Res 99:24777–24797

Loder J, Petrie B, Gawarkiewicz G (1998) The coastal ocean off northeastern north America: a large-scale view. Sea 11:105–133

Marchesiello P, McWilliams JC, Shchepetkin A (2001) Open boundary conditions for long-term integration of regional oceanic models. Ocean Model 3:1–20

Marshall J, Adcroft A, Hill C, Perelman L, Heisey C (1997) A finite-volume, incompressible Navier Stokes model for studies of the ocean on parallel computers. J Geophys Res 102:5753–5766

McDougall T (1987) Neutral surfaces. J Phys Oceanogr 17:1950–1967

Mooers CNK, Maul GA (1998) Intra-Americas Sea circulation, coastal segment(3,W). The Sea 11. Wiley New York, pp 183–208

Oey LY, Chen P (1992) A nested-grid ocean model: with application to the simulation of meanders and eddies in the Norwegian Coastal Current. J Geophys Res 97:20063–20086

Orlanski I (1976) A simple boundary condition for unbounded hyperbolic flow. J Comput Phys 21:251–269

Pain CC (2000) Brief description and capabilities of the general CFD code FLUIDITY. Internal report. Imperial College, London

Sheng J, Tang L (2003) A numerical study of circulation in the western Caribbean Sea. J Phys Oceanogr 33:2049–2069

Sheng J, Tang L (2004) A two-way nested-grid ocean circulation model for the Meso-American Barrier Reef System. Ocean Dynamics 54:232-242. DOI: 10.1007/s10236-003-0074-3

Sheng J, Thompson KR (1996) A robust method for diagnosing regional shelf circulation from scattered density profiles. J Geophys Res 101:25647–25659

Sheng J, Greatbatch RJ, Wright DG (2001) Improving the utility of ocean circulation models through adjustment of the momentum balance. J Geophys Res 106:16711–16728

Sheng J, Zhai X, Greatbatch RJ (2005) Numerical study of the storm-induced circulation on the Scotian Shelf during Hurricane Juan using a nested-grid ocean model. Prog Oceanogr (in press)

Sheng J, Wright DG, Greatbatch RJ, Dietrich D (1998) CANDIE: a new version of the DieCAST ocean circulation Model. J Atm Oceanic Tech 15:1414–1432

da Silva AM, Young CC, Levitus S (1994) Atlas of surface marine data 1994, Vol 3. Anomalies of heat and momentum fluxes. NOAA Atlas NESDIS 8, pp 413, NOAA, Washington, DC

Smagorinsky J (1963) General circulation experiments with the primitive equation. I. The basic experiment. Mon Wea Rev 21:99–165

Smith PC, Petrie B, Mann CR (1978) Circulation, variability and dynamics of the Scotian Shelf and Slope. J Fish Res Board Can 35:1067–1083

Zhai X, Sheng J, Greatbatch RJ (2004) A new two-way nested-grid ocean modelling technique applied to the Scotian shelf and slope. In: Estuarine and coastal modeling: Proceedings of the 8th international conference, pp 342–357

Zhao J, Greatbatch RJ, Sheng J, Eden C, Azetsu-Scott K (2004) Improvement in the transport of CFCs in a model of the North Atlantic that uses an adiabatical correction technique. schemes. G Res Lett 31: 10.1029/2005GL020206, L12309